PHYSICAL REVIEW D **84,** 104013 (2011)

Isotropic extensions of the vacuum solutions in general relativity

C. Molina,[1,*] Prado Martín-Moruno,[2,†] and Pedro F. González-Díaz[2,‡]

[1]*Escola de Artes, Ciências e Humanidades, Universidade de São Paulo, Av. Arlindo Bettio 1000, CEP 03828-000, São Paulo-SP, Brazil*
[2]*Instituto de Física Fundamental, Consejo Superior de Investigaciones Científicas, Serrano 121, 28006, Madrid, Spain*

(Received 22 July 2011; published 4 November 2011)

In this work, we obtain isotropic extensions of the usual spherically symmetric vacuum geometries in general relativity. Exact and perturbative solutions are derived. The classes of geometries obtained include black holes in compact and noncompact universes, wormholes in the interior region of cosmological horizons, and anti-de Sitter geometries with excess/deficit solid angle. The tools developed here are applicable in more general contexts.

DOI: 10.1103/PhysRevD.84.104013 PACS numbers: 04.70.Bw, 04.20.−q

I. INTRODUCTION

Spacetimes described by spherically symmetric solutions of Einstein's equations are of paramount importance both in astrophysical applications and theoretical considerations. And among those, black holes are highlighted. They are relevant sources of gravitational radiation, offering possible observational signatures of general relativity extensions. The current and upcoming gravitational wave experiments and the possibility of detecting black holes in accelerators are strong motivations for the investigation of such models.

In a vacuum, Birkhoff's theorem and its generalizations to nonasymptotically flat cases uniquely fix the metric as the Schwarzschild, Schwarzschild–de Sitter, or Schwarzschild–anti-de Sitter geometries, the vacuum solutions of the usual general relativity with zero, positive or negative values for the cosmological constant, respectively. Nevertheless, our universe is not in a vacuum state, even if its dynamics could principally be driven by an (at least) effective cosmological constant [1,2]. Therefore, it is interesting to consider how the compact solutions in general relativity are modified in a cosmological scenario. In a different direction, anti-de Sitter geometries gained interest due to the proposed anti-de Sitter (AdS)–conformal field theory (CFT) correspondence [3,4]. This conjecture proposes a duality between gravity in AdS spaces and CFTs. A better understanding of AdS backgrounds plays an important role in this program.

In this work, we are mainly interested in black holes in a cosmological environment. Of the two main assumptions of the cosmological principle, homogeneity is lost when compact objects are considered. Nevertheless, isotropy is still possible, and we enforce this condition. Within this context, we investigate spatially isotropic solutions close—continuously deformable—to the usual vacuum solutions.

From a more mathematical point of view, isotropy is a condition that can be implemented in a purely coordinate invariant way, and as a simple linear constraint in the usual coordinate system (t, r, θ, ϕ). This geometrical condition is somewhat akin to the imposition of a constant Ricci scalar, natural in a Randall–Sundrum brane world context [5,6]. Solutions of this constraint can also be expressed as a linear deformation of the general relativity vacuum solutions, whose extensions were treated in [7–10].

The present work deals with the problem of extending the usual Einstein's equation solutions in a similar manner. While one practical approach to general relativity is to specify the matter content and from that the spacetime structure, this is not the only possible treatment. For instance, one can specify the spacetime metric based on physical and geometrical considerations, and later follow its implications for the energy-momentum tensor [7–15]. In fact, currently, the cosmological scientific community is attempting to adjust the energy density and pressure needed to produce an accelerated FLRW cosmology. We favor here this latter approach.

The structure of this paper is presented in the following. In Sec. II, we develop the basic formalism to be used. In Sec. III, we apply this formalism, deriving linear solutions which exactly satisfy the isotropy constraint. A large class of structures appear in the process. In Sec. IV, we go beyond the linear cases, obtaining more general backgrounds which are approximately isotropic. Some final comments are made in Sec. V.

II. GENERAL FORMALISM

In this work, we are interested in spherically symmetric and static geometries. With these conditions, the metric can be written as

$$ds^2 = -A(r)dt^2 + \frac{1}{B(r)}dr^2 + r^2(d\theta^2 + \sin^2\theta d\phi^2). \quad (1)$$

In the coordinate system (t, r, θ, ϕ), the stress-energy tensor has generally the form

*cmolina@usp.br
†pra@iff.csic.es
‡p.gonzalezdiaz@iff.csic.es

$$[T^{\mu}_{\nu}] = \begin{bmatrix} -\rho & & & \\ & p_r & & \\ & & p_t & \\ & & & p_t \end{bmatrix}. \tag{2}$$

We assume spacial isotropy, that is, a linear constraint among p_r and p_t as

$$p_r = p_t \equiv p. \tag{3}$$

An eventual non-null cosmological constant is written in the Einstein equations as

$$R^{\mu}_{\nu} - \frac{1}{2}R\delta^{\mu}_{\nu} + \Lambda\delta^{\mu}_{\nu} = 8\pi T^{\mu}_{\nu}. \tag{4}$$

The field Eq. (4) implies that the stress-energy components are related with the functions A and B as

$$8\pi\rho = -\Lambda + \frac{1}{r^2} - \frac{B}{r^2} - \frac{B'}{r}, \tag{5}$$

$$8\pi p_r = \Lambda - \frac{1}{r^2} + \frac{B}{r^2} + \frac{1}{r}\frac{BA'}{A}, \tag{6}$$

$$8\pi p_t = \Lambda + \frac{1}{2}\frac{1}{r}\frac{A'B}{A} - \frac{1}{4}\frac{(A')^2B}{A^2} + \frac{1}{2}\frac{1}{r}B' + \frac{1}{4}\frac{A'B'}{A} + \frac{1}{2}\frac{A''B}{A}. \tag{7}$$

where "$'$" denotes differentiation with respect to r. The Schwarzschild ($\Lambda = 0$), Schwarzschild–de Sitter ($\Lambda > 0$), and Schwarzschild–anti-de Sitter ($\Lambda < 0$) are the vacuum solutions of the Einstein equations, trivially satisfying the condition (3) with $p_t = p_r = \rho = 0$ and an integration constant proportional to a nonvanishing M; whereas for $M = 0$, these solutions reduce to the Minkowski, de Sitter, and anti-de Sitter spacetimes. We are interested in more general solutions of Eq. (3) which are close to the Schwarzschild-like solutions, in a natural sense discussed in the following.

An equation-of-state in the form of (3), together with the Einstein Eq. (4), implies a functional relation between the functions $A(r)$, $B(r)$ and their derivatives. Using Eqs. (6) and (7), the constraint (3) can be written as

$$rAA'(-2B + rB') + 2r^2AA''B - r^2(A')^2B + 2A^2(2 - 2B + rB') = 0. \tag{8}$$

We now consider the conditions so that our solutions are continuous deformations of the usual vacuum geometries. Namely, we assume that the stress-energy tensor $T(r, \delta)$ in the form (2) is a smooth function of a deformation parameter δ such that if $\delta = 0$ we recover the vacuum solutions. We assume that the functions A and B are smooth functions of δ, but otherwise unspecified. Therefore, the stress-energy tensor (2) and the metric components can be written as

$$[T^{\mu}_{\nu}] = \sum_{n=1} \delta^n [T^{\mu}_{\nu}]_n, \tag{9}$$

$$A = \sum_{n=0} \delta^n A_n, \tag{10}$$

$$B = \sum_{n=0} \delta^n B_n. \tag{11}$$

The expansions are written so that the constant δ is dimensionless.

Substituting the form suggested by the stress-energy and metric elements in the equation of state (3), we obtain for the zero and first order in δ, respectively:

$$rA_0A_0'(-2B_0 + rB_0') + 2r^2A_0A_0''B_0 - r^2(A_0')^2B_0 + 2A_0^2(2 - 2B_0 + rB_0') = 0 \tag{12}$$

and

$$A_0(2A_0 + rA_0')B_1' - \left(\frac{4A_0^2}{r} + 2A_0A_0' + rA_0'^2 - 2rA_0A_0''\right)B_1 = -2rA_0B_0A_1'' + A_0\left(2B_0 + \frac{2rB_0A_0'}{A_0} - rB_0'\right)A_1' - \left(2rA_0''B_0 - 2A_0'B_0 + rA_0'B_0' + \frac{8A_0}{r} - \frac{8A_0B_0}{r} + 4A_0B_0'\right)A_1. \tag{13}$$

The requirement that we are dealing with extensions of the vacuum solutions sets the zero-order elements of the expansion as

$$B_0(r) = A_0(r) = 1 - \frac{2M}{r} - \frac{\Lambda}{3}r^2, \tag{14}$$

which identically solve Eq. (12). Taking into account the form of A_0 and B_0, we treat Eq. (13) writing A_1 and B_1 as

$$A_1(r) = \left(1 - \frac{2M}{r} - \frac{\Lambda}{3}r^2\right)a(r), \tag{15}$$

$$B_1(r) = \left(1 - \frac{2M}{r} - \frac{\Lambda}{3}r^2\right)b(r). \tag{16}$$

Substituting in Eq. (13), we have

$$P_1(r)b' + 6b + P_2(r)a'' + P_3(r)a' = 0 \tag{17}$$

with

$$P_1(r) = -\frac{3r}{2}(2A_0 + rA_0') = 2\Lambda r^3 - 3r + 3M \tag{18}$$

$$P_2(r) = -3r^2A_0 = r(\Lambda r^3 - 3r + 6M) \tag{19}$$

$$P_3(r) = -\frac{3r}{2}(3rA_0' - 2A_0) = 2\Lambda r^3 + 3r - 15M \tag{20}$$

At this point, the relation (17) does not fix a particular group of solutions which satisfy the isotropy condition. The complete characterization of a and b is not possible without additional information. We will develop some possible classes of solutions in the following sections.

III. EXACT LINEAR SOLUTIONS

Within the presented formalism, we will investigate exact linear solutions of spherically symmetric and isotropic geometries. They will provide a rich set of compact structures.

In addition to the already specified requirements—spherical symmetry, staticity, isotropy, and a stress-energy tensor $[T^\mu_\nu]$ in the form (9)—we will further require that $[T^\mu_\nu]$ is strictly linear in δ, that is, there are no second-order corrections. Since the exact constraint, Eq. (8), is nonlinear in A, a smooth deformation of A from A_0 by a small term δA_1 would induce higher-order corrections in $[T^\mu_\nu]$. Assuming strict linearity, and therefore excluding these higher-order corrections, implies that $A_1 \equiv 0$.

On the other hand, in terms of B the exact relation (8) is a linear first-order differential equation. Therefore, a smooth deformation of B from B_0 by an arbitrarily term δB_1 induces strictly linear corrections in $[T^\mu_\nu]$. Indeed, setting $a(r) \equiv 0$ in Eq. (17), the general solution for $b(r)$ can be obtained. We have that

$$b(r) = Db_{\text{lin}}(r) = D\exp\left(-6\int\frac{dr}{P_1(r)}\right), \tag{21}$$

where D is a dimensionless and positive integration constant. Thus, the functions $A(r)$ and $B(r)$ can be written as

$$A(r) = A_0(r), \tag{22}$$

$$B(r) = A_0(r)[1 + Cb_{\text{lin}}(r)]. \tag{23}$$

with $C = D \cdot \delta$. The specific choice of δ is a matter of convention, since it can be incorporated into C. In the present work, we will be careful to keep the constant C dimensionless.

It is straightforward to verify that the solution (22) and (23) is exact ($p_r \equiv p_t$). Both pressures will be denoted p as in Eq. (3). Although Eqs. (22) and (23) are valid for any C, we will see that the metric associated with this solution will describe static and Lorentzian manifolds for C, taking values in a proper subset of $\mathbb{R}$ only.

One common feature of the obtained spacetimes is that they are characterized by energy densities and pressures which are r-dependent, and become constant in the asymptotic region. This qualitative behavior is the expected one for compact solutions immersed in backgrounds which are asymptotically flat, de Sitter or anti-de Sitter. Excluding cosmological constant effects, this phenomenon is also seen when "hairs" are present (for example, see [16–20]). Still, the precise form and properties of the obtained geometry are strongly determined by the sign of Λ. We will treat it then case-by-case in the following subsections.

A. Linear solutions with $\Lambda = 0$

Considering a null cosmological constant, we get for the function b

$$b(r) = \frac{(r-M)^2}{M^2}, \tag{24}$$

and for the metric functions

$$A(r) = A_0 = 1 - \frac{2M}{r}, \tag{25}$$

$$B(r) = \left(1 - \frac{2M}{r}\right)\left[1 + C\left(\frac{r}{M} - 1\right)^2\right]. \tag{26}$$

In order for the geometry described by the functions A and B to have a static region (with $A > 0$ and $B > 0$), the dimensionless parameter C must be bounded from below: $-1 < C < \infty$. The energy density and pressures associated with the metric given by Eqs. (25) and (26) are

$$8\pi\rho = -C\frac{(r-M)(3r-5M)}{(Mr)^2}, \tag{27}$$

and

$$8\pi p = C\frac{(r-M)^2}{(Mr)^2}, \tag{28}$$

respectively. We also define an equation of state parameter $w = p/\rho$ which is

$$w = -\frac{r-M}{3r-5M}. \tag{29}$$

As we will show considering particular cases in the following subsections, the energy density and pressure given by Eqs. (27) and (28) would generally correspond to the total energy density and pressure which can be obtained when more than one fluid is present. Moreover, as expected from Eq. (21), one can recover the case without deformation with $C = 0$. That is, the functions resulting when $C = 0$ is taken in Eqs. (25) and (26) reduce to the Schwarzshild metric, which corresponds to the vacuum case.

1. Spatially homogeneous and isotropic universes ($M=0$)

If $M = 0$, the metric components are given by

$$A(r) = 1, \tag{30}$$

$$B(r) = 1 - Kr^2 \quad \text{with} \quad -\infty < K < \infty. \tag{31}$$

We have redefined the parameter C into a real parameter K with dimension of Length^{-2}. The metric describes a *homogeneous and isotropic background* with spacial curvature K.

It can be noted that if we consider $K > 0$, we obtain a closed static model that is the cosmological model studied by Einstein. In fact, the energy density and pressure given by Eqs. (27) and (28) can be seen as the total energy density and pressure of a universe filled with two fluids, usual matter with $8\pi\rho_m = 2K$ and a cosmological constant with $8\pi\rho_\Lambda = K$, which cancels the gravitational collapse due to the matter component. Therefore, although we are considering general relativity without cosmological constant, i.e., $\Lambda = 0$ in Eq. (4), we recover the Einstein universe as a deformation of the vacuum case with $M = 0$, the cosmological constant appears as a fluid which composes part of the universal content originated by the deformation.

An argument similar to that mentioned above could be applied to the case $K < 0$, which corresponds to an infinite static universe. Nevertheless, in this case, the fluid originated by the deformation could be decomposed into a negative cosmological constant and matter with $\rho_s < 0$ and $w_s = 0$. On the other hand, for $K = 0$, we recover the case where no deformation is considered, the Minkowski spacetime.

As we will see, the geometries presented here correspond to the asymptotic limit of the solutions with $M \neq 0$.

2. Black holes in an isotropic and noncompact universe ($M > 0$ and $C > 0$)

For positive values of C, the only zeros of the functions A and B are given by $r_+ = 2M$. Moreover, these functions are analytic and positive-definite for $r_+ < r < \infty$. Therefore, the coordinate system (t, r, θ, ϕ) is well defined in the region $r_+ < r < \infty$.

The analytic continuation beyond r_+ is possible with the standard techniques, and the surface $r = r_+$ is a Killing horizon. It is a simply connected surface for the most simple choice of topology. The interior region has a curvature singularity for $r \to 0$. On the other hand, in the limit of very large r, or equivalently taking the limit of zero mass, we obtain an static universe with a negative spacial curvature. Therefore, the resulting geometry is a *black hole in a noncompact universe*.

It must be emphasized that we have a static black hole in a nonempty environment. One possible interpretation of this geometry can be found noting that the equation of state parameter, given by Eq. (29), is equal to minus one for $r = r_+$, and that a black hole in an asymptotically de Sitter scenario would not accrete a fluid with such a value of the equation of state parameter (behaving as a cosmological constant) on its horizon [21]. Therefore, when the test-fluid approach used to study the accretion process [22] (and in Ref. [21]) is broken, the most important characteristics of the fluid are those in the vicinity of the black hole in any scenario, that is $p + \rho$ on the horizon and not at infinity. In such a case, a static configuration can be reached because a black hole would not accrete a cosmological constant, or any fluid with $w(r_+) = -1$. Nevertheless, it must be pointed out that this would be a sufficient but not a necessary nonaccretion condition.

3. Black holes in a compact universe ($M > 0$ and $-1 < C < 0$)

For negative C, that is $-1 < C < 0$, the geometry is more elaborate. The function B has a second zero $r_{\max}$ (besides $r_+ = 2M$) given by

$$r_{\max} = M\left(1 + \frac{1}{\sqrt{|C|}}\right), \tag{32}$$

such that (i) $r_+ < r_{\max}$; (ii) $A(r_{\max}) > 0$; (iii) $A(r) > 0$ and $B(r) > 0$ for $r_+ < r < r_{\max}$; (iv) $A(r)$ and $B(r)$ are analytic for $r_+ \leq r \leq r_{\max}$. As a side remark, we point out that $r_{\max}$ can be arbitrarily large, tending to infinity as C tends to zero (the Schwarzschild case), or arbitrarily close to r_+ for $|C| \to 1$ (an extremal geometry).

The surface $r = r_+$ is a Killing and outer trapping horizon, and the surface $r = r_{\max}$ is an inner trapping horizon. It can be seen that at $r = r_{\max}$ the "flaring-out condition" which characterizes wormholes [13,14], implying the existence of an outer trapping horizon [23,24], is replaced by a "flaring-in condition" for this inner horizon case. In order to understand the behavior of the geometry close to $r_{\max}$, we can consider the proper length ℓ, which is

$$\ell(r) = \pm 2M|C|^{-1/2}\eta \times \left[\frac{2|C|^{-1/2}}{|C|^{-1/2} - 1}\Pi(\mu(r), -\eta, \eta) - F(\mu(r), \eta)\right], \tag{33}$$

with

$$\eta = \frac{|C|^{-1/2} - 1}{|C|^{-1/2} + 1}, \tag{34}$$

$$\mu(r) = \arcsin\sqrt{\left(\frac{|C|^{-1/2} + 1}{|C|^{-1/2} - 1}\right)\left(\frac{|C|^{-1/2} + 1 - r/M}{|C|^{-1/2} - 1 + r/M}\right)}, \tag{35}$$

where F and Π denote the incomplete elliptic integrals of first and third kind, following the conventions in Ref. [25], and the expression for $\ell(r)$ is well defined for values of $r \geq r_+$. We have chosen a function $\ell(r)$ such that $\ell(r_{\max}) = 0$ and the $\pm$ sign in the r.h.s. of Eq. (33) analytic continues the geometry to negative values of the proper length; thus, one can use the chart (t, ℓ, θ, ϕ), with

$-\ell_{\max} < \ell < +\ell_{\max}$ and $\ell_{\max} = \ell(r_+)$ taking a finite value.

Now that we have established the good behavior of the geometry at $\ell = 0$, we can equivalently describe this extension of the space by two identical charts (t, r, θ, ϕ), both with $r_+ \leq r \leq r_{\max}$, which should be matched at $r_{\max}$. In order to visualize this geometry, we can consider that a section of our spacetime, with constant t and $\theta = \pi/2$, is embedded in an extra dimension z. Therefore, a function $z(r)$ would describe this section of the spacetime in a higher-dimensional space. The derivative of such a function would tend to infinity at r_+ and $r_{\max}$, and $z(r)$ fulfills the "flaring-in condition" in $r_{\max}$ (see Fig. 1). Thus, this maximal radius would be a surface of the same kind as that appearing in the equator of the Einstein static universe, where the light rays are parallel. In fact, one of the cases appearing in Sec. III A 1 was just the Einstein universe. It can be seen that also in that case there is an inner trapping horizon, at $r_* = (K)^{-1/2}$, which is hidden when one applies the usual change of coordinates, $r = (K)^{-1/2}\sin\eta$, in order to obtain an extension reflecting the initial geometry, which corresponds to a spatially spherical geometry, $ds^2 = -dt^2 + K^{-1}d\Omega^2_{(3)}$. On the other hand, in Fig. 2 the embedded diagram of this section of the space is depicted, showing that the geometry corresponds to a closed universe with two Killing horizons, the initial one and its reflected image, which plays the role of upper and lower limits of the figure, respectively. As in the Einstein model, the region covered by the initial chart is reflected in an identical region, closing the universe.

The Carter–Penrose diagram of the maximal extension of this geometry can be obtained by considering also values of r such that $0 \leq r \leq r_+$ for both charts, as shown in Fig. 3. As in the Schwarzschild case, for each chart, one obtains a constant radial line at $r = r_+$ which would denote the black (white) hole horizon in the upper (lower) region of the diagram, showing a connection between the corresponding line of each chart.

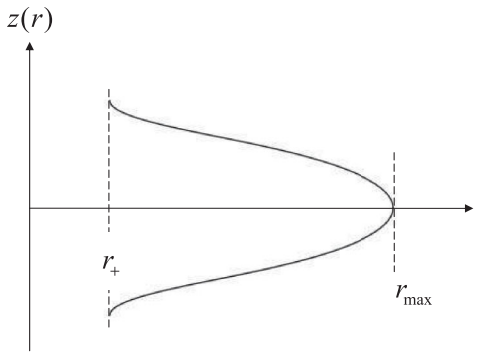

FIG. 1. Function $z(r)$ which describes the behavior of a section of the spacetime embedded in an extra dimension. It can be seen that the geometry flares in at $r = r_{\max}$.

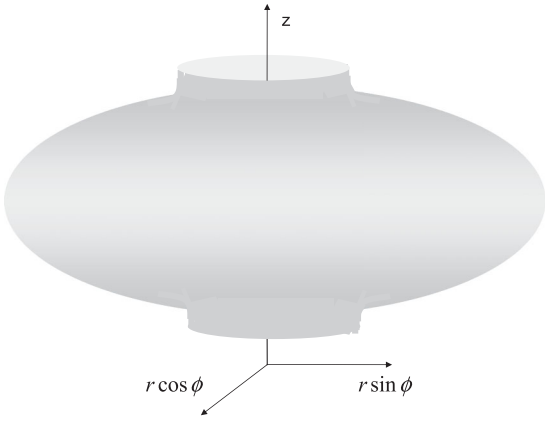

FIG. 2. Embedded diagram of a section with constant t and $\theta = \pi/2$. Both charts used to obtain this diagram have $r_+ \leq r \leq r_{\max}$, therefore the embedded diagram only shows regions with $r \geq r_+$. $r = r_+$ (top and bottom of the figure) is the limit of validity of this description.

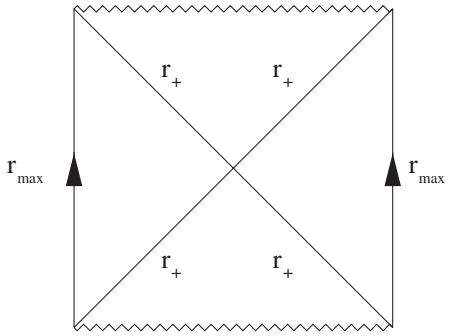

FIG. 3. Conformal diagram of the maximal extension of the considered geometry. Lines with arrows are identified. The zigzag and straight lines denote the interior singularities and the horizons, respectively.

The difference between this diagram and that of a Schwarzschild spacetime is that, in the present case, the left-hand and right-hand regions are not ending in the spatial infinity, but they are identified at a finite maximum radial radius. Therefore, whereas in the maximal extension of the Schwarzschild space, one has two asymptotically flat exterior spaces which present a black hole horizon, in this case, due to the identification at $r_{\max}$, there is only one exterior space. Assuming the maximal extension proposed, an observer in the exterior region can reach the black hole interior region by crossing two different horizons (each one parametrized by a different chart of coordinates). Thus, this geometry can be interpreted as *two black holes in a compact universe* (see Ref. [26] where a similar interpretation is considered for dynamical geometries resembling this one). A *one black hole* interpretation is also sensible, based on topological considerations.

Finally, it can be noted that the energy density, pressure and equation of state parameter, given by Eqs. (27)–(29), respectively, take finite and nonvanishing values outside

the black hole, i.e., for $r \geq r_+$. Moreover, $w(r_+) = -1$ as in the previous studied geometry (Sec. III A 2), which could be interpreted as a nonaccretion sufficient condition for an stationary solution. One could follow an argument similar to that presented in the case of the Einstein universe studied in Sec. III A 1, considering that these quantities represent the total energy density and pressure and the effective equation-of-state parameter, respectively. In such a case, a possible decomposition would be to consider one component with $w_m = 0$ and another with $w_\Lambda = -1$, although this second component would not properly be a cosmological constant because its energy density varies through the space, $\Lambda = \Lambda(r)$. Thus, one would have $\rho_m(r_+) = 0$ and $\rho_\Lambda(r_+) = |C|/(4M^2)$; and if $|C| < 1/2$, then ρ_m would start to dominate at $r_* = 3M$, whereas this radius would not be reached for $|C| > 1/2$, because $r_* > r_{\max}$.

B. Linear solutions with $\Lambda > 0$

If the cosmological constant is non-null and positive, the solutions are more complicated. If $0 < \Lambda < 1/9M^2$, then the functions $A(r)$ and $B(r)$ have two real positive roots r_+ and r_c ($r_+ < r_c$), which are the usual black hole and cosmological horizons of the Schwarzschild–de Sitter geometry, and a negative root r_-. This is the condition for the Schwarzschild–de Sitter geometry to be nonextreme, and we will assume it from now on. For $M > 0$, the polynomial $P_1(r)$ has three real zeros r_0, r_{0-}, r_n, with $r_n < 0 < r_{0-} < r_0$, and therefore can be written as

$$P_1(r) = 2\Lambda(r - r_0)(r - r_{0-})(r - r_n). \tag{36}$$

The important point is that $r_{0-} < r_+ < r_0 < r_c$. In terms of these constants, the function b can be analytically calculated as

$$b(r) = C\frac{(r - r_{0-})^{c_{0-}}}{(r - r_0)^{c_0}(r + r_0 + r_{0-})^{c_{n-}}}, \tag{37}$$

where the positive constants c_0, c_{0-} and c_{n-} are written in terms of r_0, r_{0-} and r_{n-} as

$$c_0 = \frac{3/\Lambda}{(r_0 - r_{0-})(2r_0 + r_{0-})}, \tag{38}$$

$$c_{0-} = \frac{3/\Lambda}{(r_0 - r_{0-})(2r_{0-} + r_0)}, \tag{39}$$

$$c_{n-} = \frac{3/\Lambda}{(2r_0 + r_{0-})(2r_{0-} + r_0)}. \tag{40}$$

The functions $A(r)$ and $B(r)$ are expressed as:

$$A(r) = A_0 = \frac{\Lambda}{3r}(r_c - r)(r - r_+)(r - r_-), \tag{41}$$

$$B(r) = A_0\left[1 + C\frac{(r - r_{0-})^{c_{0-}}}{(r - r_0)^{c_0}(r + r_0 + r_{0-})^{c_{n-}}}\right]. \tag{42}$$

Since the coefficient c_0 in Eqs. (38) and (42) is positive, the function $B(r)$ diverges near $r = r_0$, inside the static region $r_+ < r < r_c$. This result might suggest that the geometry might not be well-behaved if $\Lambda > 0$. Indeed, we will see in the following that this is so if $C > 0$, when a naked singularity is present. But for negative values of C, we will also see that the geometry is regular everywhere, describing a wormhole-like spacetime.

1. Naked singularities ($\Lambda > 0$ and $C > 0$)

If $C > 0$, A and B are positive-definite for $r_+ < r < r_c$. Moreover, B is divergent at r_0. The geometry is well defined and static for $r > r_0$, but its curvature invariants are not bounded, as seen by the behavior of the Kretschmann scalar near r_0:

$$\lim_{r \to r_0} |R_{\alpha\beta\gamma\delta}R^{\alpha\beta\gamma\delta}| \to \infty. \tag{43}$$

Therefore, for this case, *a naked curvature singularity* is present at $r \to r_0$.

2. Wormholes within a cosmological horizon ($\Lambda > 0$ and $C < 0$)

If $C < 0$, the function $B(r)$ is not positive-definite between r_+ and r_c: it has a third zero at $r = r_{\text{thr}}$. The relevant points are: (i) $r_+ < r_0 < r_{\text{thr}} < r_c$; (ii) $A(r) > 0$ and $B(r) > 0$ for $r_{\text{thr}} < r < r_c$; (iii) the functions $A(r)$ and $B(r)$ are analytic for $r_{\text{thr}} < r < r_c$. Therefore, the chart (t, r, θ, ϕ) is valid in the region $r_{\text{thr}} < r < r_c$. The analytic continuation of this geometry gives us a wormhole structure, with a throat at $r = r_{\text{thr}}$. The surface $r = r_c$ is a Killing horizon in the maximal extension, and can be interpreted as a cosmological horizon.

The main characteristics of this class of solutions are captured by the simpler case $M = 0$. The metric functions are given by

$$A(r) = 1 - \frac{r^2}{r_c^2}, \tag{44}$$

and

$$B(r) = \frac{(1 - r^2/r_c^2)(r^2/r_{\text{thr}}^2 - 1)}{r^2/r_0^2 - 1}, \tag{45}$$

where $r_c^2 = 3/\Lambda$, $r_0 = r_c/\sqrt{2}$,

$$r_{\text{thr}}^2 = \frac{3/\Lambda}{2(1 - |C|)}, \tag{46}$$

and C has to take values on the interval $-1/2 < C < 0$, in order that $r_{\text{thr}} < r_c$. In the limiting case $C = 0$, which corresponds to the case without deformation, one has $r_0 = r_{\text{thr}}$ and, therefore, $B(r) = A(r)$, consistently recovering the usual de Sitter metric.

The coordinate system (t, r, θ, ϕ) is valid for $r_{\rm thr} < r < r_c$. An analytic extension beyond $r = r_{\rm thr}$ can be made with the proper length ℓ as a radial function, where

$$\ell(r) = \pm \frac{2|C| r_c}{1-|C|} \Pi\left(\lambda(r), \frac{1-2|C|}{1-|C|}, \sqrt{1-2|C|}\right), \quad (47)$$

$$\lambda(r) = \arcsin\sqrt{\left(\frac{1-|C|}{1-2|C|}\right)\left(\frac{r^2 - r_{\rm thr}^2}{r^2 - r_0^2}\right)}. \quad (48)$$

We observe that the geometry described by Eqs. (25) and (26) is compact as expected, that is $-\ell_{\rm max} < \ell < \ell_{\rm max}$ with a finite value for $\ell_{\rm max}$. The function Π is the incomplete elliptic integral of a third kind, following the conventions in Ref. [25]. We have chosen $\ell(r)$ such that $\ell(r_{\rm thr}) = 0$.

Following a similar procedure to that presented in Sec. III A 3, once we have checked the good behavior of the geometry at $\ell = 0$, we can describe this extension by two identical charts (t, r, θ, ϕ), both with $r_{\rm thr} \leq r \leq r_c$. The function $z(r)$ describing the embedding of a section of this geometry in an additional dimension is shown in Fig. 4. It can be noted that this function fulfills the "flaring-out condition" and that whereas the embedding function of an asymptotically flat wormhole has a radial derivative which tends to zero for infinitely large values of r, in this case, $z(r)$ is defined only to a finite value of r, r_c, where its derivative diverges. In Fig. 5, the embedded diagram is depicted; it shows that the surface $r = r_{\rm thr}$ can be considered as a throat connecting two spatially finite spaces.

In Fig. 6, we present the Penrose–Carter diagram of the maximal extension of this geometry. It can be seen that the surface $r = r_{\rm thr}$ $(\ell = 0)$ acts as a wormhole throat and $r = r_c$ $(\ell = \ell_{\rm max})$ is the cosmological horizon. Therefore, this geometry can be interpreted as a *wormhole-like structure in an asymptotically de Sitter universe*. That is because the throat connects two universes with a cosmological horizon at $r_c = \sqrt{3/\Lambda}$ which behave as two de Sitter universes for large (but still smaller than r_c) values of r.

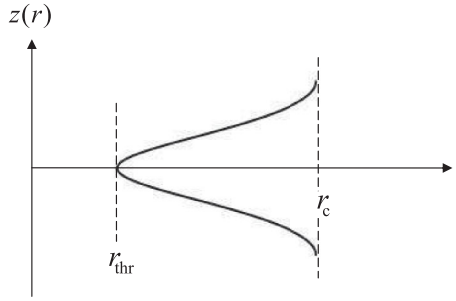

FIG. 4. Function $z(r)$ which describes the behavior of a section (with t = constant and $\theta = \pi/2$) of the spacetime embedded in an extra dimension. It can be seen that the geometry flares out at $r = r_{\rm thr}$ and that the radial derivative of $z(r)$ diverges at both $r = r_{\rm thr}$ and $r = r_c$.

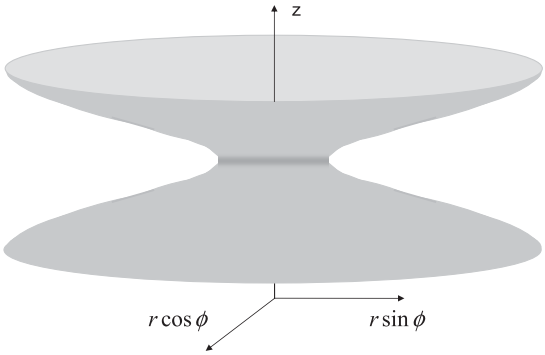

FIG. 5. Embedded diagram of a section with constant t and $\theta = \pi/2$. Both charts used to obtain this diagram have $r_{\rm thr} \leq r \leq r_c$.

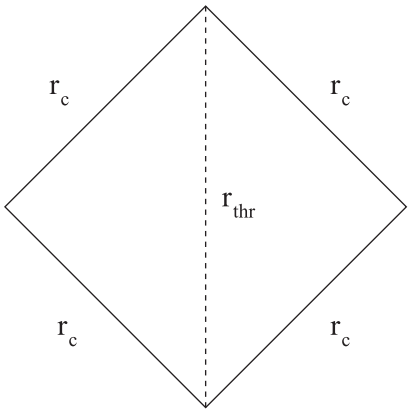

FIG. 6. Conformal diagram of the wormhole solution inside a cosmological horizon. Dashed line denotes the wormhole throat.

On the other hand, the energy density and pressure can be obtained taking into account Eqs. (44) and (45) in Eqs. (5) and (6). These are

$$8\pi\rho = -2|C|\Lambda \frac{2\Lambda^2 r^4 - 7\Lambda r^2 + 9}{(2r^2\Lambda - 3)^2}, \quad (49)$$

and

$$8\pi p = 2|C|\Lambda \frac{\Lambda r^2 - 1}{2r^2\Lambda - 3}, \quad (50)$$

respectively, leading to the equation-of-state parameter

$$w = -\frac{2\Lambda^2 r^4 - 5\Lambda r^2 + 3}{2\Lambda^2 r^4 - 7\Lambda r^2 + 9}. \quad (51)$$

These quantities are finite and nonvanishing in the interval $r_{\rm thr} \leq r \leq r_c$, and they describe matter with $\rho < 0$. On the other hand, we have $w(r_c) = -1$ and $-1 < w(r_{\rm thr}) < 0$. That is not in contradiction with the violation of the null energy condition around and on the throat of a wormhole needed to maintain such a structure (which is equivalent to the fulfillment of the flaring-out condition), since a negative energy density allows $p + \rho < 0$ having an equation

of state parameter bigger than minus one. Therefore, the fluid behaves as dual dark energy [27] around the wormhole throat and as a negative cosmological constant on the cosmological horizon. It should be kept in mind that we are considering a nonvanishing cosmological constant entering in the Einstein equations, Eq. (4), through the geometrical part; thus, it is not appearing in the material content, Eqs. (49) and (50), which vanishes for $C = 0$. Nevertheless, that is not in contradiction with a hypothetical decomposition of the material in two fluids, one of which may be a positive or negative cosmological constant. In any case, that second cosmological constant would have a different nature, because it would be originated by the deformation.

C. Linear solutions with $\Lambda < 0$

If $\Lambda < 0$, the polynomial $P_1(r)$ in Eq. (17) has one real positive root (r_0) and two complex roots. Therefore, it can be written as

$$P_1 = -\frac{6}{L^2}(r - r_0)(r^2 + pr + q), \tag{52}$$

where we have expressed the (negative) cosmological constant in terms of the AdS radius $L = \sqrt{-3/\Lambda}$, and $4q - p^2 = 3r_0^2 + L^2 > 0$. Using the previous results, we obtain for the function b:

$$b(r) = \frac{(r - r_0)^{c_0} \exp\left[-\frac{3r_0c_0}{\sqrt{3r_0^2+2L^2}} \arctan\left(\frac{2r+r_0}{\sqrt{3r_0^2+2L^2}}\right)\right]}{(r^2 + r_0r + r_0^2 + \frac{L^2}{2})^{c_0/2}}, \tag{53}$$

where

$$c_0 = \frac{2L^2}{6r_0^2 + L^2}. \tag{54}$$

The isotropic linear deformation of the Schwarzschild–anti-de Sitter geometry is given by

$$A(r) = A_0 = 1 - \frac{2M}{r} + \frac{r^2}{L^2}, \tag{55}$$

$$B(r) = A_0(r)\left\{1 + C\frac{(r - r_0)^{c_0} \exp\left[-\frac{3r_0c_0}{\sqrt{3r_0^2+2L^2}} \arctan\left(\frac{2r+r_0}{\sqrt{3r_0^2+2L^2}}\right)\right]}{(r^2 + r_0r + r_0^2 + \frac{L^2}{2})^{c_0/2}}\right\}. \tag{56}$$

Because of the complexity of this class of solutions, we initially consider the case with $M = 0$, where

$$A(r) = 1 + \frac{r^2}{L^2}, \tag{57}$$

$$B(r) = \left(1 + \frac{r^2}{L^2}\right)\left(1 + C\frac{r^2}{2r^2 + L^2}\right). \tag{58}$$

The energy density and pressure associated with this geometry are

$$8\pi\rho(r) = -C\frac{6r^4 + 7r^2L^2 + 3L^4}{L^2(2r^2 + L^2)^2}, \tag{59}$$

$$8\pi p(r) = C\frac{3r^2 + L^2}{L^2(2r^2 + L^2)}. \tag{60}$$

1. Asymptotically anti-de Sitter space with deficit/excess solid angle ($\Lambda < 0$, $M = 0$ and $C \geq -2$)

If $C \geq -2$, then the function $B(r)$ is positive-definite and the spacetime is noncompact. Its asymptotic limit is not the pure anti-de Sitter geometry though. Taking the limit $r \to \infty$, the line element can be expressed as

$$ds^2 = -\left[1 + \frac{\bar{r}^2}{\ell^2}\right]dt^2 + \left[1 + \frac{\bar{r}^2}{\ell^2}\right]^{-1} d\bar{r}^2 + (1 + C/2)\bar{r}^2 d\Omega_2 \tag{61}$$

after rescaling the radial coordinate as $\bar{r} = (1 + C/2)^{-1/2}r$ and defining $\ell = (1 + C/2)^{-1/2}L$, which is the new AdS radius. For spacetime described by Eq. (61), the solid angle of a sphere of unity radius is $4\pi(1 + C/2)$. Therefore, it presents a solid deficit or excess angle, if the sign of C is positive or negative, respectively, [28]. The asymptotic behavior shown in Eq. (61) is of a global monopole in an asymptotic anti-de Sitter spacetime [29,30].

On the other hand, the matter content which leads to this geometry, Eqs. (59) and (60), strongly depends on the sign of C. If $-2 \leq C < 0$, then this material has a positive energy density and fulfills the null energy condition in the whole spacetime.

2. Compact static universe ($\Lambda < 0$, $M = 0$ and $C < -2$)

If $C < -2$, the function $B(r)$ will have a single positive zero $r_{\max}$ given by

$$r_{\max} = \frac{L}{\sqrt{|2 + C|}}, \tag{62}$$

with $B(r) > 0$ for $0 \leq r < r_{\max}$. Analytic extension can be made with the proper length as a radial coordinate. In the maximal extension, the surface $r = r_{\max}$ is an inner trapping horizon, analogous to the already presented case in Sec. III A 3, which also in this case implies a reflection of

the geometry. Therefore, this spacetime can be interpreted as a compact static universe.

As in the previous case with $-2 \leq C < 0$, the matter content of this spacetime fulfills the null energy condition.

3. Geometries with a black hole ($M > 0$)

Considering $M > 0$, the new feature is the presence of a black hole. The functions A and B have a simple positive root at r_+, with $0 < r_0 < r_+$. The analytic extension can be made with the usual techniques and, in the maximal extension, the surface $r = r_+$ is a Killing horizon. It can also be seen that there is a curvature singularity at $r \to 0$. On the other hand, the asymptotic behavior of the spacetime depends, of course, on the value of C.

If C is positive, then the functions $A(r)$ and $B(r)$ are positive for $r > r_+$. The geometry is noncompact with asymptotic geometry described by the metric (61). As in the case $M = 0$, we observe a solid deficit angle in the asymptotic limit [28–30], whereas for smaller values of r there is a black hole. Therefore, this geometry can be interpreted as a *black hole in an asymptotically anti-de Sitter space with deficit/excess solid angle*.

For negative values of C, the function $B(r)$ has another positive root $r_{\max}$, with $r_+ < r_{\max}$ and $B(r) > 0$ for $r_+ < r < r_{\max}$. As in case discussed for $\Lambda = 0$ and $C < 0$, an analytic continuation is possible but the spacetime is compact. The resulting geometry describes an *anti-de Sitter black hole in a compact universe*.

Finally, the energy density and pressure of the fluids filling these spacetimes can be obtained by inserting Eqs. (57) and (58) in Eqs. (5) and (6). Although the obtained functions can not be expressed in a simple form, it can be seen that they are such that $w(r_+) = p(r_+)/\rho(r_+) = -1$. Therefore, our hypothesized nonaccretion condition is again fulfilled.

IV. BEYOND THE LINEAR SOLUTION

The developed formalism allows for a great deal of flexibility. We will focus here on corrections to the linear black hole solutions discussed in the previous section.

One approach to obtain more general black hole geometries, which are (approximately) isotropic, is to select an specific choice of correction function $a(r)$ which satisfies certain physical criteria. Having $a(r)$ as input, the general solution of Eq. (17) is given by

$$b(r) = Cb_{\text{lin}}(r) + b_1(r), \tag{63}$$

$$b_1(r) = b_{\text{lin}}(r) \int \frac{P_2(r)a'' + P_3(r)a'}{P_1(r)b_{\text{lin}}(r)} dr. \tag{64}$$

The polynomials P_2 and P_3 are defined in Eqs. (19) and (20). The component b_{lin} denotes the linear solution presented in Eqs. (24), (37), and (53) for null, positive, and negative cosmological constant, respectively.

With the result in Eq. (63), the general forms for A and B are

$$A(r) = A_0(r)[1 + \delta a(r)] + \mathcal{O}(\delta^2), \tag{65}$$

$$B(r) = A_0(r)[1 + Cb_{\text{lin}}(r) + \delta b_1(r)] + \mathcal{O}(\delta^2). \tag{66}$$

where A_0 is presented in Eq. (14). In Eq. (66), the constant C was redefined to absorb a δ term. We have effectively two deformation parameters: C, assuming values in an open set of the real numbers; and δ, such that $|\delta| \ll 1$ to make the perturbative expansion meaningful.

We proceed to the specification of the general form of the perturbation a. We will restrict ourselves to the case of null Λ. Extensions to $\Lambda \neq 0$ are straightforward (but somewhat cumbersome). To ensure that corrections to be introduced do not modify the global proprieties of the solutions already derived in Sec. III, we require that: (i) a should be smooth for $r \geq r_+ = 2M$; (ii) $\lim_{r\to\infty} a(r) \to 0$; (iii) a should be bounded.

Boundedness of a ensures that the perturbative approach is feasible for small enough values of δ, as will be discussed in the following. If the spacetime spatial section is noncompact, Eq. (25) gives the component $g_{tt} = -A(r)$ of the exact linear metric for $r > 2M$. Since the perturbation a is assumed to be bounded, the more general function $A(r)$ in Eq. (65) will remain positive-definite for $r > 2M$, which is a necessary condition for the staticity of the geometry. In the compact case, the linear solution for $A(r)$ is valid for $2M < r < r_{\max}$, but $r_{\max}$ can be arbitrarily large. A function $a(r)$ which remains bounded with $r_{\max} \to \infty$ ensures that the more general perturbative $A(r)$ is non-negative. Within these premises, the function $a(r)$ can be written in terms of a set of dimensionless constants $\{a_1, a_2, a_3, \ldots\}$ as an (convergent) inverse power series in the form:

$$a(r) = \sum_{n=1}^{\infty} a_n \left(\frac{M}{r}\right)^n, \tag{67}$$

with $|\delta a_n| \ll 1$. This latter condition is compatible with the requirement that the perturbation parameter δ must be small.

The linearity of the perturbative Eq. (17) allow us to solve it term-by-term. Using the results (63) and (64), the solution for $b(r)$ is given by

$$b_1(r) = \sum_{n=1}^{\infty} a_n b_{(n)}(r), \tag{68}$$

where the functions $\{b_{(n)}(r)\}$ are

$$b_{(n)}(r) = a_n \Bigg[-(-1)^n (n^2 + 9n + 14) \left(\frac{r - M}{r}\right)^2 B \times \left(-\frac{r}{r - M}; n + 2, 1 - n\right) + (2n + 7)\left(\frac{M}{r}\right)^n \Bigg], \tag{69}$$

with B in Eq. (69) being the incomplete beta function, according to the notation in Ref. [25]. To illustrate the result, the following shows the first few functions in $\{b_{(n)}\}$:

$$b_{(1)}(r) = a_1\left[\frac{24r^2 - 36Mr + 9M^2}{Mr} + 24\left(\frac{r-M}{M}\right)^2 \times \ln\left(\frac{r-M}{r}\right)\right], \tag{70}$$

$$b_{(2)}(r) = a_2\left[\frac{108r^3 - 162Mr^2 + 36M^2r + 11M^3}{Mr^2} + 108\left(\frac{r-M}{M}\right)^2 \ln\left(\frac{r-M}{r}\right)\right], \tag{71}$$

$$b_{(3)}(r) = a_3\left[\frac{300r^4 - 450Mr^3 + 100M^2r^2 + 25M^3r + 13M^4}{Mr^3} + 300\left(\frac{r-M}{M}\right)^2 \ln\left(\frac{r-M}{r}\right)\right], \tag{72}$$

$$\vdots$$

Although the series in Eq. (67) is assumed to be convergent, it is not obvious that the sum in Eq. (69) should also converge. But it indeed does, as can be seen taking the limit of large n. We have in this limit

$$\lim_{n\to\infty} \frac{b_{(n+1)}}{b_{(n)}} = \frac{a_{n+1}}{a_n}\frac{M}{r} < \frac{1}{2}\frac{a_{n+1}}{a_n} < 1, \tag{73}$$

which is a sufficient condition for convergence.

We finally point that, as required when Eq. (67) was proposed, the derived perturbation functions a and b_1 do not alter the causal and asymptotic characteristics of the linear exact function derived in the previous section.

V. CONCLUSIONS AND FURTHER COMMENTS

In this work, we have shown that the vacuum spherically symmetric geometries, Minkowski, Schwarzschild, de Sitter, Schwarzschild–de Sitter, anti-de Sitter and Schwarzschild–anti-de Sitter, can be isotropically deformed to take into account the existence of some material content. Even considering linear deformations, in the sense that the physical quantity $[T^{\mu}_{\nu}]$ is strictly linear in δ, we have obtained a zoo of geometries containing usual or exotic astronomical objects with different asymptotic behaviors.

In particular, when considering linear deformations of the Minkowski solution ($\Lambda = 0$ and $M = 0$), we have obtained spatially homogeneous and isotropic universes which are spatially closed (Einstein universe) and open, for negative and positive values of the deformation parameter (δ, which in Sec. III is included in D, with $\mathrm{sign}(\delta) = \mathrm{sign}(D)$ and, in Sec. III A 1, $\mathrm{sign}(\delta) \neq \mathrm{sign}(K)$), respectively. It is well known that, usually in order to consider those models, a cosmological constant is needed. Nevertheless, in this case the cosmological constant is not appearing through the Einstein equations, but it is part of the fluid related to the deformation.

The deformation of a Schwarzschild geometry could lead to a spacetime where a black hole is in a noncompact universe or two black holes, the original one and the reflected one, in a compact universe, depending on the sign of C (which is the same that the sign of δ). About this second solution, it must be pointed out that we have been able to obtain a closed structure with two black holes, because the deformation implies that we are no longer considering a vacuum background where Birkhoff's theorem holds (as studied in Ref. [31]).

We have also shown that both de Sitter and Schwarzschild–de Sitter spacetimes can be smoothly deformed into a geometry which can be interpreted to describe a wormhole-like structure in an asymptotically de Sitter universe if $C < 0$. Such a wormhole would consistently be supported by a material content, originated by the deformation, which violates the null energy condition on and around its throat.

The deformation of the anti-de Sitter geometry leads to a spacetime which asymptotically behaves as an anti-de Sitter space with a deficit or excess of a solid angle, or a compact static universe, depending on the value of C. A black hole should be considered in those geometries when one is deforming a Schwarzschild–anti-de Sitter space.

The above mentioned spacetimes which show the presence of black holes are examples of structures in nonvacuum spacetimes which are in equilibrium with their environment. We have noted that in all the studied cases, the fluid originated by the deformation is such that its equation-of-state parameter is equal to minus one in the black hole Killing horizon. Therefore, we have hypothesized a nonaccretion condition, in some sense inspired in Refs. [21,22], which state that a fluid which behaves as a cosmological constant on the black hole horizon would not be accreted by it. It must be emphasized that this seems to be a sufficient but not necessary condition in order to have no accretion, at least in principle.

All the geometries obtained consistently reduce to the vacuum cases when $C \to 0$. The material content originated by the deformation seems to have complicated functional forms in some of the considered backgrounds. Nevertheless, as we have seen in some cases, the energy densities and pressures can be interpreted as resulting from the sum of two or more fluids with simpler forms.

On the other hand, we have also briefly considered the application of the deformation formalism relaxing the strict isotropy constraint. As we have shown, in this case additional specifications are necessary to obtain unique solutions. We have considered possible choices of the perturbation based on physical grounds. Nevertheless, it must be pointed out that this is a powerful formalism which could provide us with new interesting solutions.

Moreover, although isotropy is the key point in the present work, extensions of usual solutions in general relativity subjected to other constraints can be explored within the same approach. For example, a constraint equation in the form $p_r = w_r\rho$ with a constant value of w_r admits as an exact linear solution (with $\Lambda = 0$)

$$A(r) = 1 - \frac{2M}{r}, \tag{74}$$

$$B(r) = 1 - \frac{2M}{r} + \frac{\delta}{r}(r - 2M)^{-1/w_r}. \tag{75}$$

A rich set of structures can be obtained for the different values of w_r taken. This constraint could be relevant in physical scenarios.

ACKNOWLEDGMENTS

This work was partially supported by MICINN (Spain) under research Project No. FIS2008-06332, CNPq (Brazil) and FAPESP (Brazil). C. Molina also thanks the kind reception by the group of *Cosmology and Gravitation* at Consejo Superior de Investigaciones Científicas, Madrid.

[1] A. G. Riess *et al.* (Supernova Search Team Collaboration), Astron. J. **116**, 1009 (1998).
[2] S. Perlmutter *et al.* (Supernova Cosmology Project Collaboration), Astrophys. J. **517**, 565 (1999).
[3] J. M. Maldacena, Int. J. Theor. Phys. **38**, 1113 (1999); Int. J. Theor. Phys. **38**, 1113 (1999).
[4] E. Witten, Adv. Theor. Math. Phys. **2**, 253 (1998).
[5] L. Randall and R. Sundrum, Phys. Rev. Lett. **83**, 4690 (1999).
[6] T. Shiromizu, K. I. Maeda, and M. Sasaki, Phys. Rev. D **62**, 024012 (2000).
[7] R. Casadio, A. Fabbri, and L. Mazzacurati, Phys. Rev. D **65**, 084040 (2002).
[8] K. A. Bronnikov and S. W. Kim, Phys. Rev. D **67**, 064027 (2003).
[9] K. A. Bronnikov, V. N. Melnikov, and H. Dehnen, Phys. Rev. D **68**, 024025 (2003).
[10] C. Molina and J. C. S. Neves, Phys. Rev. D **82**, 044029 (2010).
[11] K. A. Bronnikov, *et al.*, Phys. Rev. D **78**, 064049 (2008).
[12] Pedro F. González-Diaz and Ana Alonso-Serrano, Phys. Rev. D **84**, 023008 (2011).
[13] M. S. Morris and K. S. Thorne, Am. J. Phys. **56**, 395 (1988).
[14] Michael S. Morris, Kip S. Thorne, and Ulvi Yurtsever, Phys. Rev. Lett. **61**, 1446 (1988).
[15] Ted Jacobson, Classical Quantum Gravity **24**, 5717 (2007).
[16] Piotr Bizon, Phys. Rev. Lett. **64**, 2844 (1990).
[17] Serge Droz, Markus Heusler, and Norbert Straumann, Phys. Lett. B **268**, 371 (1991).
[18] Patrick R. Brady, *et al.*, Phys. Rev. D **55**, 7538 (1997).
[19] C. Molina, *et al.*, Phys. Rev. D **69**, 104013 (2004).
[20] S. S. Gubser, Phys. Rev. D **78**, 065034 (2008).
[21] P. Martin-Moruno, *et al.*, Gen. Relativ. Gravit. **41**, 2797 (2009).
[22] E. Babichev, V. Dokuchaev, and Yu. Eroshenko, Phys. Rev. Lett. **93**, 021102 (2004).
[23] S. A. Hayward, Phys. Rev. D **79**, 124001 (2009).
[24] P. Martin-Moruno and P. F. González-Diaz, Phys. Rev. D **80**, 024007 (2009).
[25] Gradshteyn and Ryzhik, *Table of Integrals, Series, and Products* (Academic Press, London, 2007), 7th ed..
[26] R. Nandra, A. N. Lasenby, and M. P. Hobson, arXiv:1104.4447.
[27] A. V. Yurov, P. Martin Moruno, and P. F. González-Diaz, Nucl. Phys. **B759**, 320 (2006).
[28] M. Barriola and A. Vilenkin, Phys. Rev. Lett. **63**, 341 (1989).
[29] X. Z. Li and J. G. Hao, Phys. Rev. D **66**, 107701 (2002).
[30] B. Bertrand, Y. Brihaye, and B. Hartmann, Classical Quantum Gravity **20**, 4495 (2003).
[31] J. P. Uzan, G. F. R. Ellis, and J. Larena, Gen. Relativ. Gravit. **43**, 191 (2010).